Journal of Magnetism and Magnetic Materials 9 (1978) 299–317
© North-Holland Publishing Company

MAGNETIC PROPERTIES OF LITHIUM FERRITE MICROWAVE MATERIALS *

G.O. WHITE and C.E. PATTON
Department of Physics, Colorado State University, Fort Collins, CO 80523, USA

Received 23 May 1978

This report presents a comprehensive review of the magnetic properties of lithium ferrite materials. The fundamental properties are considered first. These include crystal structure, magnetization, magnetocrystalline anisotropy, and magnetostriction. The extrinsic magnetic properties, which are related to microwave applications, are then examined. These include coercive force, remanence, and microwave loss. Finally, a systematic review of the effects of substituents, including titanium, zinc, manganese, cobalt, and bismuth, is presented.

1. Introduction

Li ferrite is becoming increasingly attractive for microwave applications, as a replacement for garnets and other spinel ferrites, and as the primary material in the development of the arc plasma fabrication technology [1,2]. The emergence of Li ferrite has resulted from successful employment of appropriate chemical substitutions including Mn, Bi, Ti, Zn and Co. The use of Mn and Bi gives acceptably low dielectric loss tangents, with good density. Ti or Zn substitutions afford a wide range of saturation inductions, from 0–5000 G, while small amounts of Co can greatly enhance the power handling capabilities of the material.

The requirements for a microwave ferrite are discussed by Baba et al. [3]. Briefly, such materials should have a low dielectric loss tangent, a low magnetic loss tangent at the operating bias field, a low coercive force, a large remanence ratio, and a large high power microwave instability threshold. A minimal variation in these parameters with variations in temperature and/or mechanical stress is also desirable.

Alternatives to Li ferrite have been primarily garnet materials for applications requiring a saturation induction of less than 2000 G, and MgMn or NiZn ferrites for applications requiring higher $4\pi M_s$ [3]. Li ferrite materials have been found to be superior to garnets with respect to stress sensitivity and cost [4]. They may also offer advantages with respect to low field magnetic loss and high power threshold [5]. In other aspects, Li ferrites appear to be at least comparable to garnets. Li ferrites also compare favorably with MgMn ferrites and have better overall loss and square loop properties than NiZn ferrites [3].

This deals with the basic intrinsic and extrinsic properties of lithium ferrite, with an emphasis on the system as a microwave material. It is intended to serve as a review of: the material, the extrinsic properties, and the effects of substituents. Part 2 will discuss the intrinsic properties, including crystal structure, magnetization, anisotropy, and magnetostriction. Part 3 will deal with so-called extrinsic properties, including hysteresis properties (coercive force and remanence) and microwave loss. Part 4 will discuss the impact of important substituents, namely titanium, zinc, manganese, cobalt, and bismuth, on the above properties.

2. Intrinsic properties of lithium ferrite

This article section is intended to serve as a brief, technical introduction to lithium ferrite. Its five subsections deal with: (1) an overview of the material, including the spinel structure, magnetic parameters, and sublattice designations, (2) the saturation magnetization at low temperature and the magnetic order, (3) the temperature dependence of the magnetization,

* Sponsored by the US Army Research Office, Grants DAAG04-75-6-0010 and DAHG29-77-G-0209.

(4) magnetocrystalline anisotropy, and (5) magnetostriction. The emphasis is on the fundamental magnetic parameters and how they are related to crystal structure, magnetic order, and substitutional effects. With a view toward the ultimate utility of lithium ferrite as a microwave material, the effects of substituents are tied directly to their impacts on the intrinsic magnetic properties of magnetization, exchange, anisotropy, and magnetostriction.

2.1. The material

Lithium ferrite belongs to a large class of ferrimagnetic spinel ferrite materials. The unit cell consists of 8 ($Li_{0.5}Fe_{2.5}O_4$) formula units. The 32 oxygen ions form an fcc structure. The interstices provide sites for the metal ions. Eight of the sites have a tetrahedral oxygen coordination and are termed "A" sites. Sixteen of these sites have an octahedral coordination and are termed "B" sites. The cation arrangement is often represented in a chemical notation such as

$$Fe^{3+}[Fe^{3+}_{1.5}Li^{1+}_{0.5}]O^{2-}_4 ,$$

where the unbracketed cations are located on A sites and the bracketed cations are on the B sites.

The super-exchange coupling between the Fe^{3+} ions is antiferromagnetic for B–B, A–A, and A–B nearest neighbor pairs. It is strongest for A–B pairs. Hence, the resulting magnetic order is that of two antiferromagnetically coupled ferromagnetic sublattices. These interactions lead to a Curie temperature of 893 K, and a saturation induction of 3750 G at 300 K.

Lithium ferrite, which has both Li^{1+} and Fe^{3+} ions on B sites, exhibits unique atomic ordering. Slow cooling through 750°C results in a regular arrangement of the B site cations. One obtains three Fe^{3+} ions followed by one Li^{1+} ion in rows along the [110] direction. Table 1 summarizes the effect of order on the magnetic properties. The Curie temperature and magnetization are not affected by the ordering. This is probably because the Fe^{3+} ion distribution between A and B sites is not affected. The B site ordering does strongly affect anisotropy and magnetostriction. In addition, the resistivity of ordered lithium ferrite has been reported to be larger than that of the disordered material by a factor of 10^3 to 10^4 [9].

The volatization of lithium and oxygen at temperatures above 1000°C can also severely affect the magnetic properties. The loss of Li_2O results in the formation of γ-Fe_2O_3 [10], which may precipitate out as α-Fe_2O_3 and thereby lower $4\pi M_s$. If oxygen is lost in excess of Li_2O, some of the ferric ions are reduced to Fe^{2+}. This results in a solid solution of Fe_3O_4 in Li ferrite, which has a larger $4\pi M_s$ than does Li ferrite. The presence of Fe^{2+} affects the anisotropy and magnetostriction in the same way as would a paramagnetic substituent. The presence of Fe^{3+} and Fe^{2+} ions on octahedral sites also leads to a valence exchange process which affects the resistivity and the microwave losses. West and Blankenship [9] have attributed decreases in resistivity by as much as 10^4 to this mechanism.

2.2. Saturation magnetization at zero temperature

The molecular field model is reasonably successful in relating intrinsic magnetization to chemical compo-

Table 1
Magnetic properties of pure lithium ferrite in the ordered and disordered states

State	Curie temperature T_c (K)	Saturation induction $4\pi M_S$ (G)	Crystalline anisotropy $K_1 \times 10^{-3}$ (erg/cc)	Magnetostriction coefficients $\lambda_{100} \times 10^6$	$\lambda_{111} \times 10^6$
Ordered	893	3750	−80 [a] −83 [b]	−24.2 [a] −22.4 [c]	3.9 [a] 5.9 [c]
Disordered	893	3750	−88.3 [a] −90 [b]	−28.7 [a] −32.0 [c]	2.7 [a] 2.0 [c]

[a] After Arai and Tsuya [6].
[b] After Folen [7].
[c] After Petrakovskii and Smokotin [8].

sition for Li ferrites. In this model, the exchange fields for the A and B sublattices may be written as

$$H_{ex}^{(A)} = \lambda_{AA} M_A + \lambda_{AB} M_B ,$$

$$H_{ex}^{(B)} = \lambda_{AB} M_A + \lambda_{BB} M_B ,$$

where the λ_{AA} and λ_{BB} are the intrasublattice molecular field coefficients and λ_{AB} is the intersublattice molecular field coefficient. These coefficients are generally negative for spinels. In pure lithium ferrite, these coefficients obey the relation

$$\lambda_{BB} \approx \tfrac{1}{4}\lambda_{AA} \approx \tfrac{1}{6}\lambda_{AB} < 0 ,$$

which is consistent with the ferrimagnetic ground state described in section 2.1.

Substituents can play important roles in determining the magnetization. The effects at zero temperature may be divided into three categories: (1) direct replacement of Fe^{3+} on an A or B sublattice by the substituent ion, (2) replacement with a resulting redistribution of Fe^{3+} ions among the A and B sublattices, and (3) a change in the ferrimagnetic spin structure. The amount of iron replaced is dictated by the valence of the substituent and is given by

$$M^{2+} : Li^{1+}_{0.5(1-x)} Fe^{3+}_{2.5-0.5x} M^{2+}_x O^{2-}_4 ,$$

$$M^{3+} : Li^{1+}_{0.5} Fe^{3+}_{2.5-x} M^{3+}_x O^{2-}_4 ,$$

$$M^{4+} : Li^{1+}_{0.5(1+x)} Fe^{3+}_{2.5-1.5x} M^{4+}_x O^{2-}_4 .$$

The extent of iron redistribution depends on the specific nature of the substituent ion. Changes in spin structure may occur for particular resultant Fe^{3+} distributions.

Substitutions of diamagnetic Zn^{2+} and Ti^{4+} provide specific examples of these mechanisms. With Zn^{2+}, the site distribution is believed to be [11]:

$$Zn^{2+}_z Fe^{3+}_{1-z-y} Li^{1+}_y [Li^{1+}_{0.5-1/2z-y} Fe^{3+}_{1.5+1/2z+y}] O^{2-}_4 .$$

The predicted magnetization is shown in fig. 1 as a function of Zn content [12]. It is consistent with the data of Gorter [13] for $z < 0.2$. In the case of Ti^{4+} additions, an assumed site distribution of

$$Li^{1+}_{0.5x} Fe^{3+}_{1-0.5x} [Li^{1+}_{0.5} Fe^{3+}_{1.5-x} Ti^{4+}_x] O^{2-}_4$$

is in reasonable agreement with experimental magnetization data up to $x \approx 1$ [12,14].

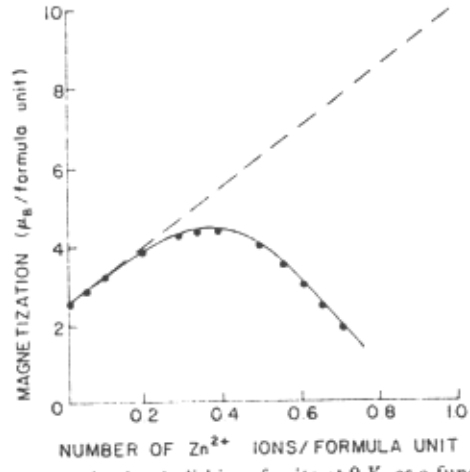

Fig. 1. Magnetization in lithium ferrite at 0 K, as a function of Zn substitution. The data points represent the extrapolated data of Gorter [13] and the dotted line, the theory without canting. (After Dionne [12].)

The magnetizations of Li ferrites with Zn^{2+} concentrations greater than 0.2 ions per formula unit, or with Ti^{4+} concentrations greater than 1 ion per formula unit, deviate from expectations based simply on the replacement and redistribution of Fe^{3+}. Similar behavior has been reported for other Zn substituted ferrites [13]. This may be explained by a change in the spin structure in which spins on a sublattice cant with respect to each other [15–18], thereby lowering the magnetization of that sublattice. With Zn substitution, canting of B sublattice spins is expected to result from an increase, due to replacement and redistribution of Fe^{3+}, in the antiferromagnetic B–B exchange molecular field relative to the normally dominant antiferromagnetic A–B exchange molecular field. The existence of spin canting in Li ferrite has yet to be verified [20]. However, canting has been observed in NiZn [21,22] and CoZn [23] ferrites, which are similar to Li ferrite.

An alternate explanation for the effects of large Zn substitution in Li ferrite has been offered by Young and Smit [19]. They propose that canting does not exist. Rather, the spins of B site Fe^{3+} ions with less than two A site Fe^{3+} nearest neighbors, are antiferromagnetically aligned with other B site spins.

2.3. Temperature dependence of the magnetization

The net magnetization and Curie temperature are functions of the molecular field parameters λ_{AA}, λ_{BB}

and λ_{AB}, and the sublattice magnetizations. The exact equations are rather involved. When the intersublattice exchange λ_{AB} dominates, one obtains a Curie temperature which depends on the number of Fe ions on the A and B sites, N_A and N_B, and the intersublattice exchange λ_{AB}:

$$T_c \propto (N_A N_B)^{1/2} \lambda_{AB} .$$

In general, substitutions will diminish all factors and reduce the Curie temperature. For lithium ferrite, the exchange coefficients and sublattice magnetizations are such that the compensation point and related magnetic behavior found in some spinels and garnets do not occur.

Molecular field exchange parameters have been reported for Li ferrite [24] and for LiTiZn ferrite [12]. The molecular field theory, with these parameters, predicts values of $4\pi M_s$, as a function of temperature, which are in good agreement with experimental data. Prince [25], however, has reported some discrepancy between observed and theoretical temperature dependences of the sublattice magnetizations in Li ferrite. He has concluded that this discrepancy is characteristic of the molecular field theory.

2.4. Magnetocrystalline anisotropy

The magnetocrystalline anisotropy free energy for a cubic crystal may be written as [26]

$$F_K = K_1(\alpha_1^2\alpha_2^2 + \alpha_2^2\alpha_3^2 + \alpha_3^2\alpha_1^2) + K_2(\alpha_1^2\alpha_2^2\alpha_3^2) ,$$

where K_1 and K_2 are the first and second order anisotropy constants, and the α_i are direction cosines of the vector magnetization relative to the crystallographic axes.

Experimental data [7] on the first order crystalline anisotropy constant K_1 for ordered and disordered pure lithium ferrites are shown in fig. 2. The solid lines in the figure represent a fit to the Yosida–Tachiki single ion anisotropy theory [27–29]. This model provides a good fit to the data, and the single ion mechanism appears to adequately explain the magnetocrystalline anisotropy in most ferrites and garnets [30,31].

It is worhtwhile to consider briefly the essentials of the model. It bears directly on both the anisotropy and magnetostriction in lithium ferrite, and the impact of substituents on these properties. The cubic term in the

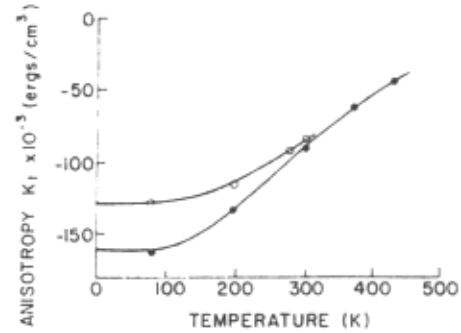

Fig. 2. Temperature dependence of K_1 in $Li_{0.55}Fe_{2.45}O_4$ for ordered (circles) and disordered (dots) states. The theory is represented by the solid lines. (After Folen [7].)

Yosida–Tachiki theory demonstrates the important features. It is

$$K_1(T) = \sum_i N_i K_{1i}(T)$$

where the i subscript enumerates different magnetic species on the A and B sites, the N_i represent the relative concentrations of each species, and the K_{1i} are the single ion anisotropy constants of each species. The temperature dependences of the $K_{1i}(T)$ are given by [29,32]:

$$\frac{K_{1i}(T)}{K_{1i}(0)} = I_{9/2}\{\mathcal{L}^{-1}[M_i(T)/M_i(0)]\} ,$$

where $I_{9/2}$ is the reduced hyperbolic Bessel function of order 9/2 and $\mathcal{L}^{-1}$ is the inverse Langevin function of the normalized sublattice magnetization. The essential features of the single ion theory are: (1) the individual sublattice contributions to the anisotropy simply add, in much the same way that the sublattice magnetizations add, and (2) the individual sublattice anisotropy contributions depend on the sublattice molecular field, so that the temperature dependence of K_1 is governed by the same considerations that yield $M_s(T)$.

These factors have important implications for the effect of substitutions on anisotropy. Diamagnetic substituents will simply modify the Fe content for the sublattices. This in turn, affects the sublattice contributions to the anisotropy, as well as the sublattice moments and the temperature dependence of those moments. Zinc, for example, enters the A sublattice and reduces the corresponding sublattice anisotropy and magnetization. At low temperature, this enhances the

dominant negative contribution from the B sublattice and K_1 becomes even more negative. At room temperature, however, the situation is reversed and K_1 becomes less negative [33]. This is due to the effect of the zinc on the temperature dependence of both sublattice magnetizations [34].

Paramagnetic substituents constitute distinct magnetic species within the single ion model. Thus, in addition to their effects on the iron distribution, paramagnetic substituents can make a direct single ion contribution to the anisotropy. For certain paramagnetic substituents, the single ion contribution can be large. The temperature dependence of this contribution will depend upon the exchange coupling of the substituent moment to the iron sublattice magnetizations, and, in general, will differ from the temperature dependences of the A and B site Fe^{3+} contributions. The effects of Co^{2+} substitution in Li ferrite exemplify the single-ion contribution of a paramagnetic substituent [35–37]. Less than 0.006 atoms per formula unit of Co are required to reverse the sign of the 0 K anisotropy in Li ferrite. As expected, the effect on K_1 is proportional to the Co concentration. The Co contribution to K_1 also decreases rapidly with increasing temperature. With 0.006 atoms per formula unit of Co, this results in a compensation point in K_1 at about 150 K. A systematic survey of the effect of various substituents on anisotropy will be presented in part 4 of this work.

2.5. *Magnetostriction*

Magnetostriction and magnetocrystalline anisotropy in ferrites have much in common: (1) the parameters have complex temperature variations, (2) phenomenological formulations are often utilized, and (3) the single-ion formalism appears applicable to both. The magnetostrictive free energy is written as [26]:

$$F_\sigma = \tfrac{3}{2}\sigma\lambda_{100}(\alpha_1^2\gamma_1^2 + \alpha_2^2\gamma_2^2 + \alpha_3^2\gamma_3^2) + 3\sigma\lambda_{111}(\alpha_1\alpha_2\gamma_1\gamma_2 + \alpha_2\alpha_3\gamma_2\gamma_3 + \alpha_3\alpha_1\gamma_1\gamma_3).$$

Here, λ_{100} and λ_{111} are the commonly measured magnetostriction coefficients, the α_i are direction cosines of the magnetization as before, the γ_i are the direction cosines of the stress, and σ is the magnitude of the stress.

Data on the temperature dependence of λ_{100} and λ_{111} for lithium ferrite have been reported by Petrakovskii and Smokotin [8]. Their results are shown in fig. 3. Ordering decreases $|\lambda_{100}|$ and increases $|\lambda_{111}|$. The solid lines represent theoretical fits based on the single-ion theory [38]. The temperature dependences of the sublattice magnetizations used in the fits were taken from the neutron diffraction data of Prince [25]. When the single-ion theory is applied to magnetostriction, one obtains a sublattice magnetostriction contribution which is given by,

$$\lambda^A(T)/\lambda^A(0) = I_{5/2}\{\mathcal{L}^{-1}[M_A(T)/M_A(0)]\}.$$

It is essentially this approach which yielded the fits shown in fig. 3. Thus, single-ion theory appears to adequately explain both anisotropy and magnetostriction.

As with anisotropy, the molecular field dependence of the magnetostriction constants leads to complications in the prediction of substitutional effects at nonzero temperature. This is exemplified by the case of Zn substitution, which is reported to reduce the room temperature $|\lambda_{100}|$ [33]. Based solely on the Fe^{3+} site redistribution, an increase in $|\lambda_{100}|$ is expected. Birss and Isaac [39] provide an excellent survey of the theoretical basis of magnetostriction in magnetic oxides and a review of ferrite data. A systematic survey of the

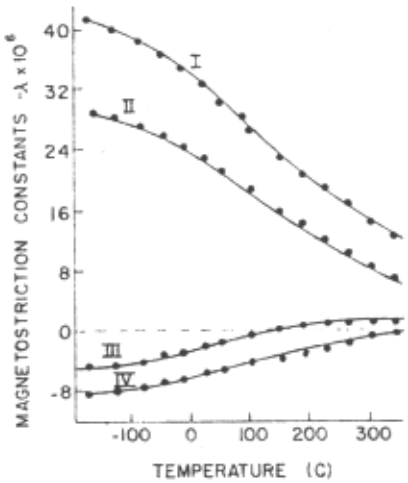

Fig. 3. Temperature dependence of the magnetostriction constants of pure single crystal lithium ferrite, in ordered and disordered states. Data set I: λ_{100} (disordered); data set II: λ_{100} (ordered); data set III: λ_{111} (disordered); data set IV: λ_{111} (ordered). The solid lines are based on the single-ion theory as discussed in the text. (After Petrakovskii and Smokotin [8].)

effects of substituents on magnetostriction in Li ferrite will be provided in part 4 of this work.

3. Extrinsic properties of lithium ferrite

Part 2 reviewed intrinsic, microscopic properties which are primarily associated with single crystals. Part 3 considers "extrinsic" magnetic properties which describe the interaction of the material with external fields. These properties include (1) hysteresis loop properties, such as remanence and coercive force, which are related to low frequency magnetization processes, and (2) microwave properties, such as the FMR linewidth, effective linewidth, and spin-wave linewidth, which are related to the high frequency relaxation processes. Such properties depend on microstructural considerations such as grain size and porosity, electrical properties, and materials processing factors, as well as the intrinsic parameters.

3.1. Magnetization processes and coercive force

Remagnetization and hysteresis phenomena are of considerable importance to both microwave [3] and computer [40] applications of Li ferrite materials. Square hysteresis loops, low coercive force, and large remanence are most desirable. These properties can vary with temperature and can be altered by chemical substitution. The following brief discussion of hysteresis will serve as a basis for understanding the effects of temperature and compositional variation on the coercive force and remanent magnetization.

Magnetization reversal in ferrites occurs primarily by the irreversible growth of reverse domains [41,42]. Such growth will occur at an applied field for which the net energy of the system is lowered by an increase in domain volume. In homogeneous grains, the decrease in volume magnetostatic energy must be greater than the increases in the domain wall energy and magnetostatic energy of the domain surface. The domain wall energy is given by

$$\sigma_\omega \sim [A(K_1 + \lambda_i \sigma)]^{1/2} ,$$

where A is the micromagnetic exchange parameter, K_1 is the crystalline anisotropy, and $\lambda_i \sigma$ is the stress anisotropy. The surface magnetostatic energy which couples domains in adjacent grains is given by

$$\sigma_{ms} \sim M_s^2 \langle(\cos\theta_1 - \cos\theta_2)^2\rangle ,$$

where M_s is the saturation magnetization and θ_1 and θ_2 are the angles between the magnetization within each grain and the normal to the grain boundary. The coercive force due to the domain wall energy is [41]:

$$H_c^{(wall)} \sim \sigma_\omega / M_s a_0 ,$$

where a_0 is the average grain diameter. The magnetostatic contribution is [41]:

$$H_c^{(ms)} \sim M_s \langle(\cos\theta_1 - \cos\theta_2)^2\rangle .$$

These two considerations alone lead to a coercive force of

$$H_c = C_1 \sigma_\omega / M_s a_0 + C_2 M_s .$$

The lithium ferrite data of Schwabe and Campbell [43] in fig. 4 are consistent with the above equation. The values $C_2\sigma_\omega/M_s = 16.97$ and $C_2 M_s = 0.88$, which fit the data, indicate that the wall energy term is dominant for these samples. An inverse dependence on grain size has also been observed in crystalline nickel [41], and in YIG. For YIG, the C_2 or magnetostatic contribution appears to be negligible [42].

Polycrystalline microwave ferrites contain stress gradients and magnetic anomalies such as pores which

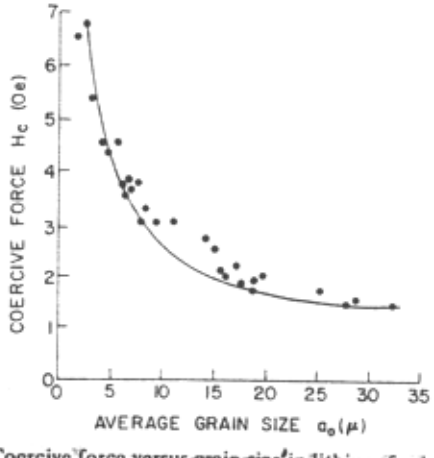

Fig. 4. Coercive force versus grain size in lithium ferrite. The data are from Schwabe and Campbell [43]. The solid curve indicates a fit to the phenomenological equation, $H_c = A_1/a_0 + A_2$, with $A_1 = 16.97$ and $A_2 = 0.881$.

contribute to the domain wall and magnetostatic energy terms, and hence to the coercive force. Based on dynamic effects in Ni ferrite [44] and Mg ferrite [45], Baldwin [46,47] has shown that porosity can locally alter one or both of these terms. Theoretical analyses of such effects [41,42,48] differ in detail, but agree that porosity should increase the coercive force. Experimental results confirm this general tendency but the scarcity of systematic data precludes the identification of specific mechanisms. Stress can also affect coercive force. Considerable effort has been expended with regard to these relationships [41,42,49–52]. Particular models differ substantially in detail, but all relate stress to coercive force, through the effects of stress on the domain wall and/or magnetostatic energies. In each case, the stress sensitivity of the coercive force is expected to depend on the effect of stress on the dominant energy term. Thus, the relationship between stress and coercive force may be very different for different materials, and for different stress distributions. For example, uniform stress has been found to increase the coercive force in MgMn ferrite [51], but to decrease the coercive force in permalloy 68 [50]. Data on the stress sensitivity of Li ferrites are limited. However, as shown in fig. 5, a stress relief anneal appears to substantially reduce the coercive force in an arc plasma deposited LiTiZn ferrite.

The effect of a given intrinsic parameter such as anisotropy, magnetostriction, or $4\pi M_s$, on the coercive force is determined by the role of that parameter in the domain wall and magnetostatic terms, and upon the relative magnitudes of these terms. Depending upon the particular situation, varying chemical composition or temperature may produce either an increase or a decrease in H_c. The effects of such changes must therefore be assessed on a case-wise basis. A summary of possible correlations appears in table 2. The effects of specific substituents are discussed in part 4.

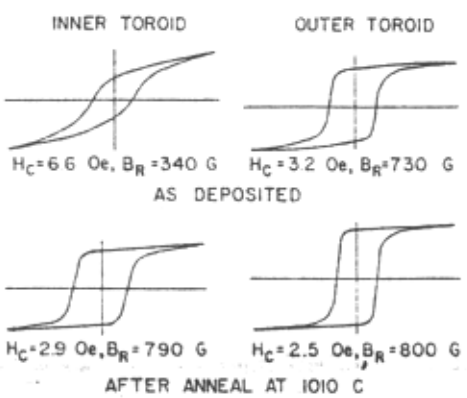

Fig. 5. Effect of stress relief anneal on the hysteresis properties of LiTi ferrite. (After Babbitt [1].)

3.2. Remanent magnetization

The mechanisms by which a saturated or partially magnetized ferrite relaxes to the remanent state are as important as those of magnetization processes and the coercive force. The problem here, however, is more of domain wall nucleation than of propagation.

In the absence of reverse domain nucleation, the magnetization within each grain will simply relax by rotation to the nearest easy direction, which is determined by the net effect of crystalline anisotropy, magnetostrictive and magnetostatic interactions. For pure crystalline anisotropy, the spins are expected to lie within a cone of solid angle $\Omega = \pi/2$, which corresponds to a remanence ratio $R \equiv M_r/M_s$ of 0.87 [53]. However, random stress and dipolar fields, which tend to reduce R, are almost always present.

Some degree of domain structure is probably present at remanence, and is also likely to play a role in determining R [9]. Reverse domains may result from incomplete domain propagation during magnetization [42], or may consist of spike domains nucleated on magnetic inhomogeneities [54,55] or on grain boundaries [41,56]. In either case, the nucleation and volume of these domains are determined by equation of the driving surface dipolar energy with the opposing energy required to create or expand the domain wall.

Stress gradients can affect the remanence, both through alteration of the relaxation cone angle [51, 57] and through effects on reverse domain nucleation and volume [58]. Both effects are predicted to depend upon the ratios of λ_{100}/K_1 and λ_{111}/K_1. Stress sensitivity through alteration of the relaxation cone angle is expected to vanish for λ_{100} approximately equal to $-0.4\,\lambda_{111}$, while that due to alteration of spike domain volume is expected to vanish for λ_{100} equal to $1.5\,\lambda_{111}$. Both effects appear to be important in YIG [57]. In Li ferrite however, their roles have yet to be conclusively demonstrated [35].

Table 3 summarizes the important processes that contribute to remanence, as related to intrinsic mate-

Table 2
Summary of factors affecting coercive force in polycrystalline ferrites

Contribution	Effect(s)	Effect on H_c
Exchange	increase domain wall energy	increase
Magnetization	promote domain growth in a magnetizing field	decrease
	increase dipolar fields due to magnetization discontinuities at grain boundaries, stabilize spike domains against growth in a magnetizing field	increase
Anisotropy	increase domain wall energy	increase
	moderate wall pinning due to localized stress	decrease
	moderate effect of random stress on H_c (ms) by reducing the average angle of M_s across a grain boundary	decrease
Magnetostriction and stress	uniform stress can increase the domain wall energy	increase
	uniform stress can promote magnetization alignment across grain boundaries, and reduce dipolar fields	decrease
	stress may increase the variation in the potential in which the wall moves	increase
	nonuniform stress can increase the average angle of M_s across a grain boundary, which increases H_c (ms)	increase
Porosity	pores may pin domain walls	increase
Grain size	domain size ∝ grain size; driving term in H_c proportional to 1/domain size	decrease

rial properties and microstructure. The fact that particular contributions may either increase or decrease remanence, depending on the details of the process, emphasizes the complexity of the problem. On the other hand, the various connections make it possible to identify the particular processes involved on an empirical basis. Stress relief in lithium ferrite, for example, can increase the remanence as shown in fig. 5 in the last section [1]. This indicates that the first two factors listed under magnetostriction in table 2 are most relevant.

3.3. Microwave loss in single crystals

The microwave properties of lithium ferrite are of fundamental and practical importance. The microwave relaxation yields information on the interactions between magnetic excitations and the crystal lattice. Such relaxation may be separated into two categories: (1) processes which are operative in single crystals, and (2) processes which are related to polycrystallinity and microstructural considerations. This section focuses on the first category, so-called intrinsic losses. Impurity and defect contributions are also considered. The next section examines microwave loss in polycrystals.

The two basic microwave parameters which serve to characterize the microwave loss in single crystals are the FMR (ferromagnetic resonance) linewidth ΔH and the spin-wave linewidth ΔH_k. Both are generally observed to increase with frequency and to exhibit temperature dependences which reflect the interactions between the magnetic excitations and the lattice. The details are involved and rather specialized. A readable treatise on the subject has been written by Sparks [59].

The temperature dependences of the FMR and spin-wave linewidths in single crystal Li ferrite at 5.2 GHz [60] are shown in fig. 6. A temperature peak contribution is observed, superimposed on a contribution which is proportional to temperature. The linear contribution is due to long-range interactions and represents the

Table 3
Summary of factors affecting remanence in polycrystalline ferrites

Contribution	Effect(s)	Remanence effect
Exchange	increases wall energy and inhibits nucleation	increase
Magnetization	increases stray fields, widens cone angle, and promotes nucleation	decrease
Anisotropy	sign of K_1 determines the easy axes and size of cone angle for noninteracting, single domain crystallites	
	increased K_1 can overcome stress and demagnetizing stray fields to narrow the cone angle	increase
	increased K_1 increases the domain wall energy and inhibits reverse domain nucleation	increase
	a large K_1 may also increase the nucleation tendency of spike domains on pores	decrease
Magnetostriction and stress	random stress can increase the cone angle	decrease
	random stress, in increasing the cone angle, can increase the stray fields at grain boundaries and promote domain nucleation	decrease
	uniform stress can reduce the cone angle	increase
	uniform stress can, in reducing the cone angle, reduce the stray fields at grain boundaries and decrease nucleation	increase
	uniform stress can increase the wall energy and inhibit nucleation	increase
Porosity	increases stray fields, widens cone angle, promotes nucleation	decrease

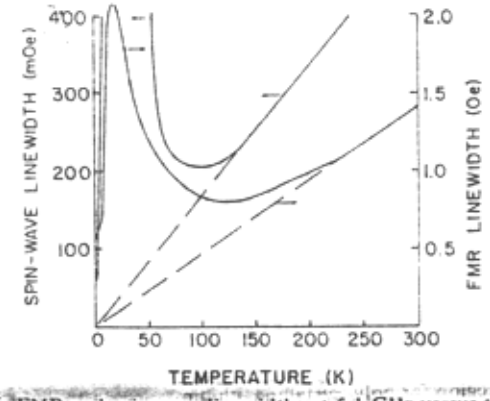

Fig. 6. FMR and spin-wave linewidths at 5.1 GHz versus temperature for single crystal lithium ferrite. (a) FMR linewidth; (b) spin-wave linewidth at $k = 0$. (After Spencer et al. [60].)

"intrinsic" linewidth. The temperature peak is indicative of impurity relaxation [59]. The data of Nilsen [61] suggest that the impurity process in Li ferrite may be classified as a "fast relaxation" process. It is probably due to Fe^{2+} [11,62]. A temperature peak has also been observed in Co doped Li ferrite [63]. Here, however, the temperature peak is due to Co^{2+} and the process appears to be of the "slow relaxation" type.

More complete characterization of the intrinsic relaxation processes in Li ferrite may be obtained from the wave-number dependence of the parallel pumping spin-wave linewidth. Data of Petrakovskii and Berzhanskii [64] are shown in fig. 7. The spin-wave linewidth at zero wave number, $k = 0$, is about 0.85 Oe. The theoretical magnon–phonon scattering linewidth is 0.5 Oe. There is probably some contribution due to three-magnon processes as well at $k = 0$. The k dependence is approximately linear, with a reasonable fit to

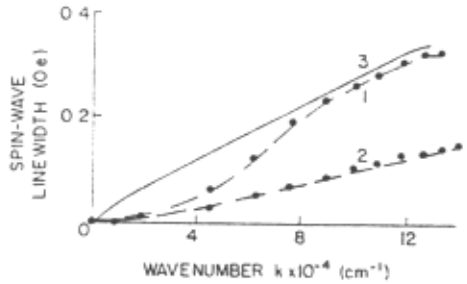

Fig. 7. Wavenumber dependence of the parallel pumping spin-wave linewidth $\Delta H_k - \Delta H_{k\to 0}$ at 9.2 GHz and 520 K, for ordered (curve 1) and disordered (curve 2) lithium ferrite single crystals. Curve 3 is a theoretical prediction based on three magnon confluence. (After Petrakovskii and Berzhanskii [64].)

a three-magnon confluence process as shown by curve 3 in the figure. A two-magnon scattering contribution is also evident from the nonlinear k dependence at low k for the ordered crystal. The data are consistent with the calculation of Sage [65] for two-magnon influences on ΔH_k. Berzhanskii and Petrakovskii [66] report similar results and conclusions for Al substituted Li ferrite.

Relaxation processes in Li ferrite appear also to be order and defect sensitive. Spencer and Denton [67] report a three-fold increase in the FMR linewidth due to B site disordering. Lepore et al. [68] report a substantial linewidth increase due to microscopic structural defects. However, as shown in fig. 7, the spin-wave linewidth decreases in disordered single crystals.

In summary, pure single crystal lithium ferrite exhibits an intrinsic linewidth which is in accord with theoretical calculations based on multimagnon–phonon processes. It is linear in frequency and temperature, and is on the order of 1 Oe at room temperature. Superimposed on this variation is an impurity peak contribution which is of importance primarily at cryogenic temperatures. This contribution may fall into the category of fast relaxation or slow relaxation, depending on the impurity. Small residual amounts of Fe^{2+} appear to act as fast relaxation contributions. Other paramagnetic ions may have similar effects on the microwave loss in Li ferrite. An essential point is that the intrinsic linewidth is small, the lowest reported for spinels.

3.4. Microwave losses in polycrystals

All of the processes considered in section 3.3 for single crystals apply as well to polycrystals. In addition, the polycrystallinity and microstructure can increase the microwave loss in various ways. The increases fall into two general categories: (1) effects of microstructure on the ferromagnetic resonance losses, and (2) effects of microstructure on the relaxation mechanisms at very low or very high bias fields far from resonance.

In Li ferrite polycrystalline materials, the ferromagnetic resonance linewidth is generally hundreds of Oe, as compared to 1 Oe in single crystals. Fig. 8 shows the effective linewidth ΔH_{eff} versus magnetic field near resonance for arc plasma sprayed LiTi ferrites with $4\pi M_s \approx 1200$ G [69]. The value of ΔH_{eff} at the resonance field of 3.5 kOe corresponds approximately to the conventional FMR linewidth. These data are qualitatively explained by porosity and anisotropy induced inhomogeneity broadening and two-magnon scattering [70,71].

FMR data on polycrystalline Li ferrite containing large amounts of Ti and Zn are shown in fig. 9 [72]. Of particular note are the relatively low linewidths, and the linewidth minima as functions of composition. The latter suggest the possibility of a compensation point in K_1, with a consequent null anisotropy contribution to the linewidth.

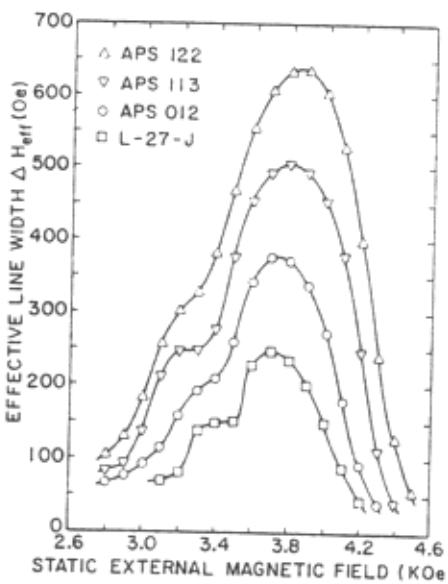

Fig. 8. Effective linewidth as a function of static external field in the two-magnon scattering region for polycrystalline lithium ferrite at 10 GHz and 300 K. The lowest curve is for conventionally fired Trans Tech L-27-J. The other data are for arc plasma sprayed materials. (After Kaelberer et al. [69].)

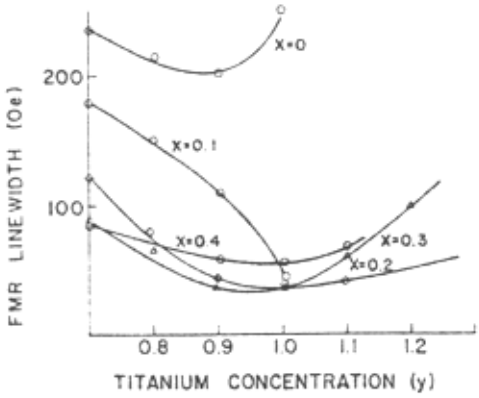

Fig. 9. Ferromagnetic resonance linewidth in TiZn substituted lithium ferrite at X-band and 300 K, where y denotes the number of Ti atoms per formula unit and x denotes the number of Zn atoms per formula unit. (After Konwicki and Makolagwa [72].)

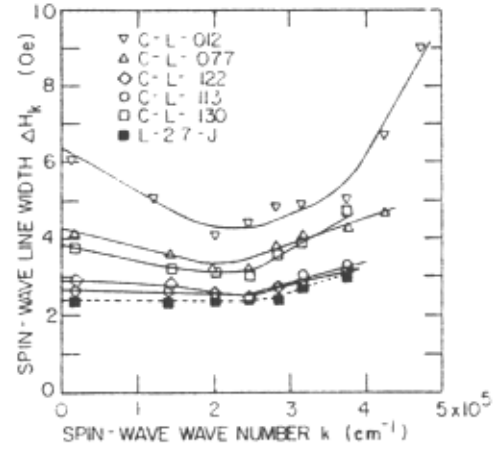

Fig. 10. Spin-wave linewidth ΔH_k versus wavenumber k for parallel pumping at 9.2 GHz and 300 K for 1200 G Ti substituted Li ferrite. (After Kaelberer et al. [69].)

The second category of losses in polycrystals consists of the losses far from resonance. The spin-wave linewidth ΔH_k is one measure of such losses. The coupling between degenerate spin waves does not appreciably influence ΔH_k in typical coarse grained polycrystalline ferrites [73]. It is also possible to extend effective linewidth measurements out of the near resonance, two-magnon scattering region. These off-resonance effective linewidths are not influenced by the processes responsible for microstructure related FMR line broadening.

Fig. 10 shows data on the spin-wave linewidth ΔH_k at 8.9 GHz and room temperature versus wave number for parallel pumping. A conventionally fired LiTi ferrite with $4\pi M_s \approx 1200$ G is shown (TransTech L-27-J) along with data on several arc plasma materials. The most important feature of the data is the relatively small values of the ΔH_k, as compared with the resonance and near resonance linewidths in figs. 8 and 9. The extrapolated values at $k = 0$ range from 2.5 Oe to 6.5 Oe. These spin-wave linewidths are comparable to those in polycrystalline YIG. The values are somewhat larger than the single crystal data of the last section. The k-dependences are more complicated and are probably related to grain-size effects.

Fig. 11 presents data on the off-resonance effective linewidth at 10 GHz and room temperature for LiTi ferrite with $4\pi M_s \approx 1200$ G. The values of ΔH_{eff} at fields above 5 kOe, and at a low field of about 2 kOe, are comparable to the ΔH_k values. These off-resonance linewidths of 5–10 Oe are substantially smaller than the FMR linewidth. They are comparable to off-resonance ΔH_{eff} data for polycrystalline YIG and are somewhat larger than Li ferrite single crystal linewidths.

In principle, the off-resonance effective linewidths and the spin-wave linewidths in coarse-grain polycrystalline ferrites should be the same as those in single crystals, with values on the order of 1 Oe. In practice they are generally larger as the above data show. Although the specific reasons for the differences are not

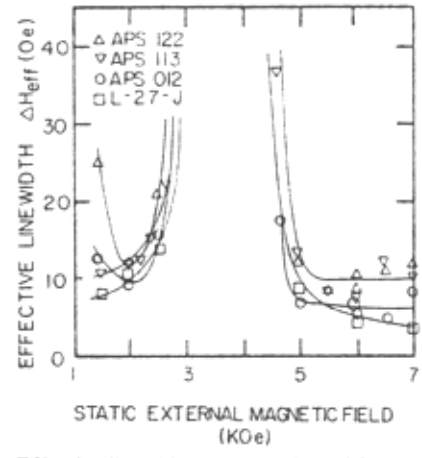

Fig. 11. Effective linewidth as a function of field outside the spin-wave manifold region for Ti substituted Li ferrite at 10 GHz and 300 K. The data are for a conventionally fired (L-27-J), and for arc plasma (APS) materials. (After Kaelberer et al. [69].)

understood, they appear to be related to the microstructure.

Fig. 12 shows spin-wave and low-field effective linewidths as functions of temperature for several LiTi and LiTiCo ferrites with $4\pi M_s \approx 2250$ G. The fact that ΔH_k is independent of temperature, and other data [69,73,74], suggest that ΔH_k in polycrystalline Li ferrite is largely determined by microstructural mechanisms. Microstructure also appears to play a role in determining ΔH_{eff} [73–75]. However, the significant temperature dependence of ΔH_{eff} shown in fig. 12 suggests that other factors are also important. One such possibility involves the magnetostriction [75,76].

In summary, microstructure makes significant contributions to microwave relaxation in Li ferrite. The data of Kaelberer et al. [69] show the qualitative correlations. The specific microstructural considerations, at present, derive from more extensive studies on YIG. Further data on Li ferrite materials, with systematic variations in microstructure and magnetostriction, as a function of temperature are needed to pinpoint the processes which are important in this system.

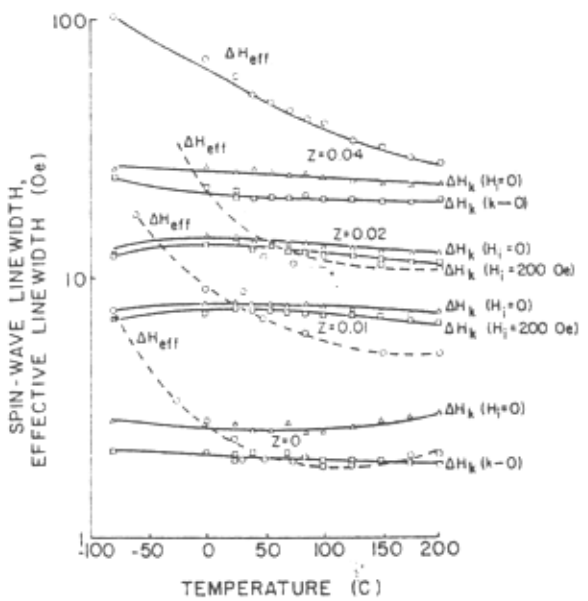

Fig. 12. Spin-wave linewidth ΔH_k and effective linewidth ΔH_{eff} at 9.2 GHz, versus temperature for Co substituted LiTi ferrites with saturation induction of 2250 G. Cobalt concentration in atoms per formula unit is indicated by z. (After Green and Van Hook [5].)

4. The effect of substituents

Parts 2 and 3 have presented a survey of the intrinsic and extrinsic magnetic properties of lithium ferrite. Part 4 will provide a systematic review of the effects of important substituents on these properties. The specific substitutions which are discussed are important for lithium ferrite as a microwave material.

4.2. Titanium substitutions

Substitution of Ti^{4+} in Li ferrite reduces the saturation magnetization. For Ti concentrations less than one ion per formula unit, the decrease in zero temperature magnetization is nearly proportional to the Ti concentration. This is consistent with replacement and redistribution of Fe^{3+} ions. The results of larger Ti substitutions are shown in fig. 16. The departure from linearity suggests that spin canting (cf. section 2.2) is present at high Ti concentrations. The temperature dependence of the magnetization as a function of Ti concentration, based on molecular field calculations with canting not included, is shown in fig. 13. Titanium reduces the temperature dependence of the magnetization. The curves of fig. 13 were generated [12] by choosing exchange parameters which afforded fits of magnetization data at 0 K, 300 K, and T_c. Both inter and intrasublattice

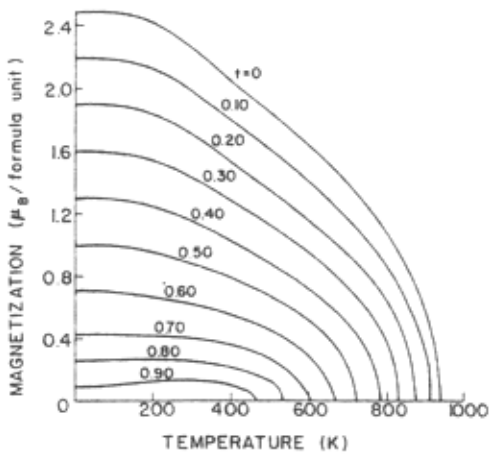

Fig. 13. Theoretical magnetization curves for Ti substituted lithium ferrite. The vertical axis is in Bohr magnetons per formula unit. The t parameter denotes the number of Ti atoms per formula unit. (After Dionne [12].)

exchange parameters were found to decrease in magnitude with increasing Ti concentration.

Low level Ti^{4+} substitution reduces both K_1 and λ_{100}, while λ_{111} is increased [33]. Lithium ferrite single crystals with titanium content greater than 0.1 atoms per formula unit have not yet been grown, so that data in this range for anisotropy and magnetostriction are not available. In view of the importance of such materials for low frequency microwave applications, single crystals with large titanium additions would be quite useful for fundamental measurements.

The extrinsic properties do not seem to be affected to any great degree by Ti additions. Baba et al. [3] report an increase in coercive force and decrease in remanence, but the effects are small for less than 0.6 atoms of Ti per formula unit. These small changes are, however, consistent with an increase in the misalignment of magnetization from grain to grain. Due to absence of single crystal anisotropy and magnetostriction data, a quantiative analysis of the changes in terms of micromagnetic parameters is not warranted at the present time.

4.2. Zinc substitutions

As with Ti^{4+}, Zn^{2+} alters the magnetization by replacement and redistribution of Fe^{3+}. As discussed in section 2.2, the net result is a reduction in the amount of Fe^{3+} on the A sublattice, and an increase in the amount of Fe^{3+} on the B sublattice. For Zn concentrations of less than 0.35 atoms per formula unit, Zn additions (cf. fig. 1) increase the zero temperature $4\pi M_s$. The decrease in magnetization with higher Zn levels may be indicative of a change in magnetic order, as discussed in section 2.2. Zinc is also reported [12] to decrease the exchange parameters λ_{AB} and λ_{BB}, while increasing λ_{AA}. The resulting decrease in T_c, combined with the increase in zero temperature $4\pi M_s$, results in an increase in the temperature dependence of the magnetization, as is shown in fig. 14.

The effects of Zn additions on anisotropy and magnetostriction are shown in table 4. These data indicate that small levels of Zn addition decrease $|K_1|$ and $|\lambda_{100}|$. This is not expected on the basis of site preference, but is plausible if the temperature dependences of both sublattice contributions are considered [34]. Yakovlev et al. [11] report the temperature dependence of the anisotropy field (K_1/M) to be insensitive to Zn additions between −200°C and 300°C.

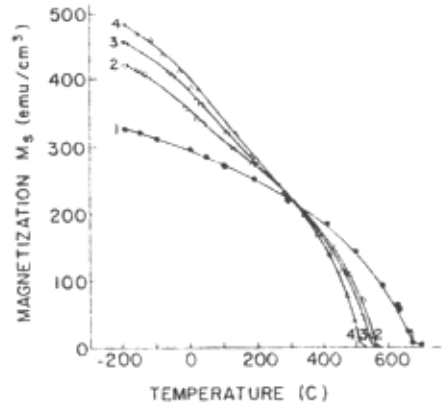

Fig. 14. Saturation magnetization M_s versus temperature for Zn substituted lithium ferrite up to $z = 0.24$ atoms per formula unit. Curves 1, 2, 3 and 4 are for 0.0, 0.1, 0.18, and 0.24 atoms of zinc per formula unit, respectively. (After Yakovlev et al. [11].)

Zinc addition has also been reported [9] to affect the microstructural properties of hot pressed, annealed Li ferrites. As shown in fig. 15, the bulk density increases linearly with Zn substitution. The porosity, on the other hand, increases with Zn up to 0.1 atoms per formula unit, but decreases for greater concentrations.

Low level Zn additions have been found to improve the hysteresis and microwave properties of Li ferrites. For substitutional levels up to 0.3 atoms per formula unit, West and Blankenship [9] report that Zn additions simultaneously decrease H_c and increase R. Arc plasma spayed LiTi ferrites show the same effects [77]. The decrease in coercive force may be due to the decrease in the anisotropy contribution to the domain wall energy. The increase in R may be due to a decreased tendency for spike domain nucleation which is also due to the decrease in K_1 [58].

Zn additions appear to reduce the microwave losses. Davydov et al. [78] report that Zn substitution at 0.65 atoms per formula unit reduces the low field loss by a factor of four. Zn addition is also reported to decrease the near resonance ΔH_{eff} [9,69] in polycrystalline Li and LiTi ferrites, and the resonance linewidth in single crystal Li ferrite [11]. The decreases in low field loss and ΔH_{eff} are consistent with the decrease in anisotropy, the increase in density, and the reduction in porosity cited above. The reduction in single crystal reso-

Table 4
Effects of Zn substitution on the room temperature magnetization, anisotropy, and magnetostriction in Li ferrite (after Dionne [33])

Composition	Magnetization $4\pi M_s$ (G)	Anisotropy $K_1 \times 10^{-3}$ (erg/cm^3)	Magnetostriction $\lambda_{100} \times 10^6$	$\lambda_{111} \times 10^6$
$Fe^{3+}_{1.0}[Li^{1+}_{0.5}Fe^{3+}_{1.5}]O_4$	3750	−90.4	−25.8	2.3
$Fe^{3+}_{0.8}Zn^{2+}_{0.2}[Li^{1+}_{0.4}Fe^{3+}_{1.6}]O_4$	4602	−67.7	−22.4	4.5
$Fe^{3+}_{0.36}Zn^{2+}_{0.64}[Li^{1+}_{0.18}Fe^{3+}_{1.82}]O_4$	2658	−26.5	−11.1	2.3

nance linewidth has been attributed to a reduction in the residual Fe^{2+} with Zn additions [11].

4.3. Simultaneous Ti–Zn additions

Ti and Zn are employed together for many low frequency microwave applications. As noted above, the Ti is used to lower $4\pi M_s$, and may be present in large concentrations. Zn is typically present at levels of less than 0.1 atoms per formula unit and is added to improve hysteresis and microwave properties. As with LiTi ferrite, single crystal data on K_1, λ_{100} and λ_{111} do not exist. However, at typical concentrations, the combined substituent effects on device properties are consistent with the available data for LiTi and LiZn ferrites [3].

The effects of large simultaneous substitutions of Ti and Zn on magnetization and Curie temperature [72] are shown in figs. 16 and 17. The behavior is more complicated than one would predict, based on the effect Zn or Ti substitution alone. As shown in fig. 16, the addition of Zn destroys the linear relationship between $4\pi M_s$ and Ti concentration. Fig. 17 shows that Zn addition causes T_c to increase with increasing Ti concentration between 0.9 and 1.1 atoms per formula unit. This behavior might be attributed to a change in spin structure (cf. section 2.2).

Such heavily doped materials have yet to be utilized in device applications, but they do exhibit promising microwave properties. For example, Konwicki and Makolagwa [72] report a substituted material with $4\pi M_s$ of 500 G and a resonance linewidth of only 30 Oe at 10 GHz.

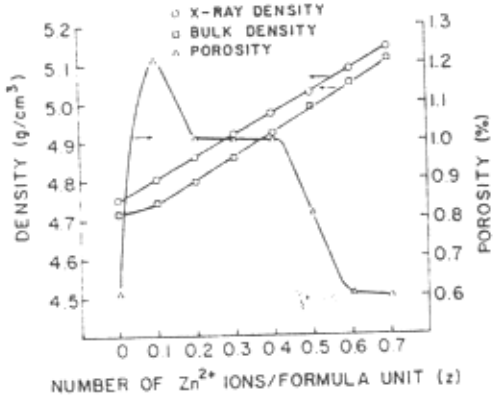

Fig. 15. Bulk density, volume fraction porosity, and X-ray density versus Zn content (z is the number of Zn ions per formula unit) for Li ferrite with Zn additions. The materials were hot pressed at 1175°C for $\frac{1}{2}$h, annealed at 980°C for 4 h, and cooled at 10°C/h at 300°C. (After West and Blakenship [9].)

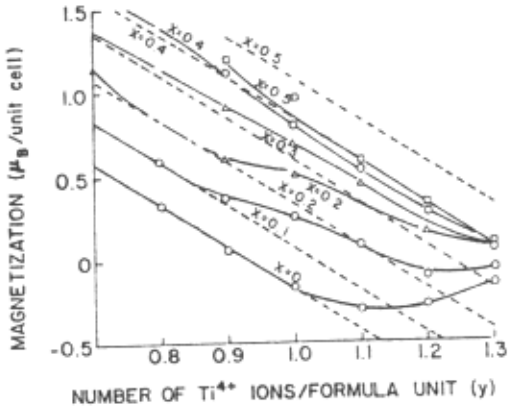

Fig. 16. Magnetic moment at 0 K, in μ_B per unit cell, for LiTiZn ferrite as a function of y, the number of Ti ions per formula unit, and x, the number of Zn ions per formula unit. (After Konwicki and Makolagwa [72].)

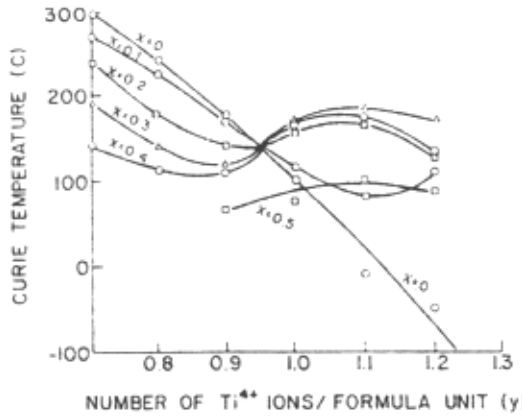

Fig. 17. Curie temperature as a function of y, the number of Ti ions per formula unit, and x, the number of Zn ions per formula unit, for LiTiZn ferrite. (After Konwicki and Makolagwa [72].)

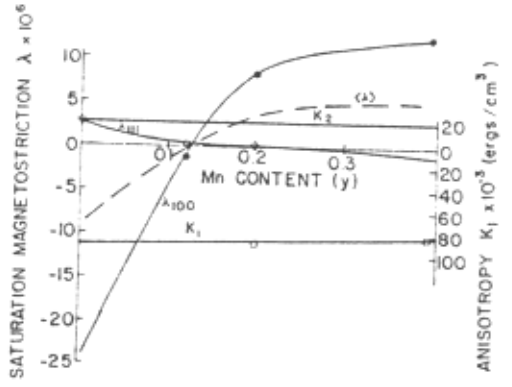

Fig. 18. Room temperature magnetostriction and magnetic anisotropy parameters as a function of Mn content y in $Li_{0.5}Mn_yFe_{2.5-y}O_4$ single crystals. (After Van Hook and Dionne [35].)

4.4. Manganese substitutions

Small amounts of Mn^{3+} are added to microwave Li ferrites, to ensure an acceptably low dielectric loss tangent. The Mn^{3+} is expected to reside on the B sites [79]. Because octahedrally coordinated Mn^{3+} is a Jahn–Teller ion, clustering of Mn^{3+} can occur even at low levels of substitution [80]. This clustering disrupts the 1 : 3 ordering of Li^{1+} and Fe^{3+} on the B sites, and is believed to displace some Li^{1+} to the A sites [80–82].

Manganese additions can alter the intrinsic magnetic properties of Li ferrite. The effects on K_1, λ_{100} and λ_{111} in single crystals of Li ferrite are shown in fig. 18. Sufficient Mn^{3+} addition changes the sign of λ_{100} and reduces $|\lambda_{111}|$, but has little effect on K_1. Mn addition is also reported to increase $4\pi M_s$ and to reduce T_c [3, 81,82]. The increase in $4\pi M_s$ is surprising, because the magnetic moment of Mn^{3+} is less than that of Fe^{3+} which it replaces. An increase in $4\pi M_s$ is consistent, however, with displacement of Li to the A sites [81, 82].

The effects of Mn^{3+} in polycrystalline Li ferrite may differ from those in stoichiometric single crystals, because polycrystalline Li ferrite inevitably contains some Fe^{2+}. The ferrous ion will yield a positive single ion contribution to λ_{111} [35,40], increase $4\pi M_s$, and greatly increase the conductivity. In Li ferrite, Fe^{2+} is oxidized by Mn^{3+} according to the reaction [83]:

$$Fe^{2+} + Mn^{3+} \rightarrow Fe^{3+} + Mn^{2+} .$$

The resulting Mn^{2+} is expected to magnetically similar to Fe^{3+}. Therefore, the observed affects of small manganese additions to polycrystalline Li ferrite may be due in part to a reduction in residual Fe^{2+}.

Interaction of Fe^{2+} and Mn^{3+} may be manifested by the increase in $4\pi M_s$ reported [81,82] for Mn additions at levels which are too low to cause lithium displacement. The following argument assume that Fe^{2+} and Mn^{3+} contribute four μ_B per ion to the magnetization, where μ_B is the Bohr magneton, whereas Fe^{3+} and Mn^{2+} contribute five μ_B per ion. Each Mn^{3+} replaces an Fe^{3+} one for one, which results in a loss of one μ_B per ion. However, the oxidation of Fe^{2+} and consequent reduction of Mn^{3+} may be expected to result in a gain of two μ_B. Thus, each substituted Mn^{3+} ion which is subsequently reduced is expected to increase the magnetization by one μ_B. Other effects of the $Mn^{3+} - Fe^{2+}$ interaction are noted in the following paragraphs.

Manganese addition alters the hysteresis properties of Li ferrite. The reported effects vary according to Mn concentration and the presence of other substituents. Manganes additions of up to 0.1 atoms per formula unit to Li ferrite have been reported [35,82] to decrease H_c, but to have little effect on R and the stress sensitivity of R. On the other hand, increasing Mn concentration from 0.4 to 0.6 atoms per formula unit has been reported [84] to increase H_c and decrease R. Small Mn additions have also been reported [82] to substantially reduce the amount of hysteresis loop degradation due to Co substitution. The lack of correla-

tion between Mn doping and the stress sensitivity of R has been attributed to the oxidation of Fe^{2+} [35]. The other effects are probably related to the effect of Mn^{3+} on the magnetostriction, the oxidation of Fe^{2+}, and/or the clustering of octahedral Mn^{3+} [80]. More specific conclusions regarding the mechanisms do not appear warranted by existing data.

Manganese reduces the conductivity and microwave dielectric loss tangent by the oxidation of Fe^{2+} [3]. Van Hook and Green [82] have reported reductions of four orders of magnitude in both conductivity and dielectric loss tangent at 10 GHz, for Mn addition at 0.1 atoms per formula unit. The effects of Mn additions on the microwave magnetic properties of Li ferrite have not been studied in detail. However, the oxidation of Fe^{2+} is expected to diminish the low temperature peak in the intrinsic linewidth [85]. A linear relationship between ΔH and ΔH_k and Mn^{3+} concentrations has been reported [85] in single crystals of Mn ferrite. Consequently, Mn additions to polycrystalline Li ferrite might result in increases in ΔH_{eff} and ΔH_k.

4.5. Cobalt substitutions

Very low levels of Co substitution have been found to have considerable effect on K_1, λ_{100}, λ_{111}, R, H_c, ΔH, ΔH_{eff} and ΔH_k in lithium ferrite. These effects have been attributed to Co^{2+} on the B sites. In the low concentrations normally used, Co^{2+} has little effect on $4\pi M_s$ or T_c.

The effects on K_1, λ_{100} and λ_{111} are shown in figs. 19 and 20. Cobalt additions produce compensation points in λ_{111} and K_1, but simply increase λ_{100} [33, 36,37,86]. It is noteworthy that Ti^{4+} additions appear to nullify the effects of Co on K_1 [82,87].

Cobalt additions have been reported to greatly affect the hysteresis properties of Li ferrite [5,35,82]. Data on coercive force and remanence are shown in fig. 21. These data show that Co additions cause sharp increases in H_c and decreases in R with decreasing temperature. This behavior has been attributed to the effect of Co in producing a compensation point in K_1. As shown in fig. 19, the compensation point shifts to higher temperature as the Co concentration is increased. Cobalt substitution has also been reported [5] to substantially increase H_c and decrease R in LiTi ferrites of $4\pi M_s \approx 1200$ G. The nature of these effects is not clear, since Co is not believed to affect K_1 in the presence of Ti substitution.

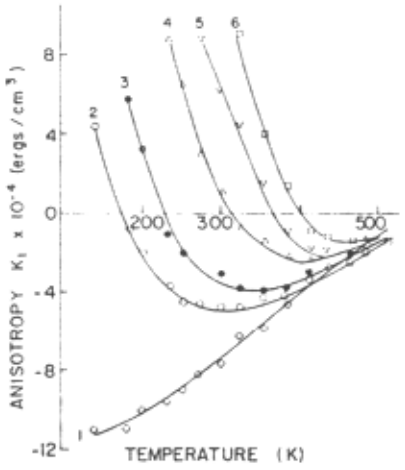

Fig. 19. Anisotropy constant K_1 versus temperature for cobalt substituted Li ferrite. Curves 1, 2, 3, 4, 5 and 6 correspond to 0.0, 0.006, 0.009, 0.015, 0.026 and 0.035 atoms per formula unit, respectively. (After Stel'mashenko [36].)

Cobalt additions also have large effects on the microwave properties of Li ferrite. As discussed in section 3.3, Co increases the intrinsic linewidth through a "slowly relaxing" impurity mechanism. This mechanism is evident in Co doped polycrystalline Li ferrite, where both ΔH_k and the low-field loss at room temperature are reported [3,5,82] to increase linearly with increasing Co concentration. Bunina et al. [88] report that the correlation between ΔH_k and Co concentration is enhanced by the concurrent presence of Zn. Cobalt

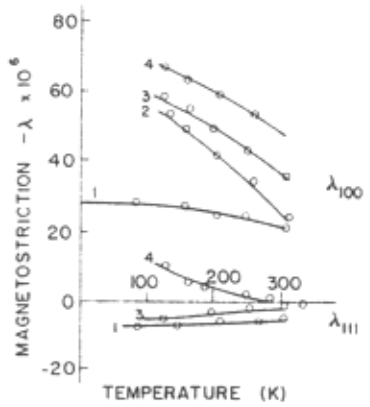

Fig. 20. Magnetostriction constants λ_{100} and λ_{111} versus temperature for cobalt additions in lithium ferrite. Curves 1, 2, 3 and 4 correspond to 0.0, 0.003, 0.0035 and 0.044 atoms of Co^{2+} per formula unit. (After Protopopova et al. [86].)

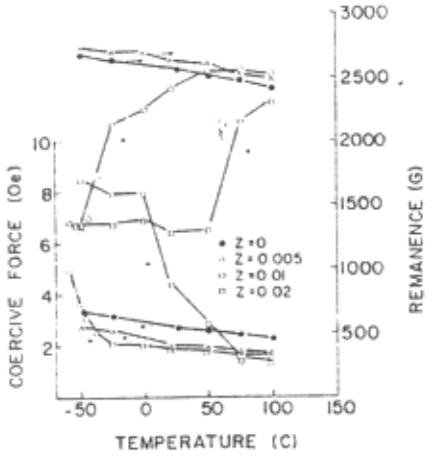

Fig. 21. Effect of cobalt additions (z atoms per formula unit) on coercive force and remanence in Li ferrite as a function of temperature. (After Van Hook and Dionne [35].)

doping also affects the FMR linewidth, but here the primary effect is through K_1. Banerjee et al. [87] report that a minimum in the room temperature FMR linewidth occurs at Co concentration of 0.015 atoms per formula unit which, as shown in fig. 19, produces a compensation point in the room temperature value of K_1.

4.6. Bismuth addition

Bismuth is employed in lithium ferrite as flux to enhance densification at lower firing temperatures which are expected to minimize lithium and oxygen loss in polycrystalline Li ferrite and thereby to minimize the creation of Fe_2O_3 and Fe^{2+} (cf. section 2.1). Bismuth is also reported to promote pore migration to the grain boundaries [89] and the growth of large grains [82].

Bismuth would appear to affect the intrinsic properties only indirectly as it inhibits the formation of Fe^{2+} or Fe_2O_3. To the extent that it inhibits Fe^{2+} formation, Bi will minimize the attendant increases in λ_{111}, $4\pi M_s$, and conductivity. To the extent that it inhibits the formation of Fe_2O_3, Bi addition will minimize the decrease in $4\pi M_s$ due to the precipitation of α-Fe_2O_3.

Bismuth additions have been found to decrease coercive force [3,82]. This is probably due to an increase in grain size. Bismuth is also reported to reduce the dielectric loss tangent, due to reduction of Fe^{2+} concentration. It should be noted, however, that this effect is not of sufficient magnitude to render Mn addition unnecessary.

5. Summary

Through the employment of appropriate substituents and through the variation of the microstructure, polycrystalline Li ferrite can be suited to a wide range of microwave applications. Substituents commonly found in microwave Li ferrites include Ti, Zn, Mn, Co, and Bi. The effects of these elements on the hysteresis and microwave properties have been considered in terms of their effects on intrinsic parameters such as magnetization, crystalline anisotropy, and magnetostriction, and the relationships of these parameters to the hysteresis and microwave properties. The effects of other substituents might be similarly anticipated.

The effects of a substituent on the magnetization, anisotropy, and magnetostriction can be understood in terms of the molecular field theory and the single-ion model. The theory is relatively simple and straightforward, and is quantitatively successful in certain instances such as that of Co substitution. However, its application requires knowledge of the valence, the site preference, and of the magnetic properties of the substituent ion on the preferred site. The theory is therefore of less quantitative utility where these factors are complicated by the presence of other ions. Examples of such cases are that of Mn addition where the valence of Mn is ambiguous due to the presence of Fe^{2+}, and that of Co^{2+} addition in which the single ion anisotropy due to Co^{2+} is apparently diminished by the concurrent presence of Ti^{4+}. Application of the theory can also be complicated by substitution of e.g. Ti and/or Zn at levels which are sufficiently large as to alter the spin structure.

The mechanisms by which the intrinsic parameters and the microstructure govern the hysteresis properties are not as well defined as the relationships between substituents and the intrinsic parameters. The theories of hysteresis are legion, but which if any is entirely appropriate to Li ferrite has not been clearly established. The coercive force appears to vary inversely with grain size and to increase with porosity, although the exact nature of the porosity dependence is not clear. The relationships between the coercive force and the intrin-

sic parameters have yet to be unambiguously identified. However, it is likely that the anisotropy and magnetostriction affect the coercive force primarily through their effects on the domain wall energy. The magnetization is most important as it contributes to the volume magnetostatic energy. The mechanisms affecting remanence appear to have been identified for other polycrystalline ferrites such as YIG, but the importance of these mechanisms in Li ferrite has not yet been verified.

The mechanisms of microwave relaxation in polycrystalline Li ferrite are also largely unknown. Notable exceptions are the cases of dielectric relaxation and near-resonance magnetic relaxation. Dielectric relaxation is due largely to the presence of Fe^{2+}. Near-resonance relaxation in polycrystalline ferrites including Li ferrite is due to inhomogeneity broadening and two-magnon scattering. As with other polycrystalline ferrites, however, the relaxation mechanisms at bias fields far from resonance have yet to be identified. Nevertheless, increasing grain size and decreasing porosity are expected to lower both the effective and spin-wave linewidths. Increases in the effective and spin-wave linewidths are known to result from the substitution of single ion relaxers such as Co^{2+}.

Further development of Li ferrite can be expected to result from the use of other substituents, and from microstructural optimization. Such development would be greatly facilitated by better understanding of the correlations between microstructural and intrinsic parameters, and hysteresis and microwave properties. Greater understanding of the combined effects of multiple substitutions would also be desirable.

Acknowledgements

The authors are indebted to many colleagues in the field of microwave materials for helpful comments, advice, and information during the preparation of this review. Gerald Dionne, Tom Collins, Richard Babbitt, Russ West, Jerry van Hook, Jerry Green, and Paul Baba are gratefully acknowledged for their assistance in this regard. We would also like to thank Charles Brower for reading the manuscript.

References

[1] R.W. Babbitt, IEEE Trans. Magnetics 11 (1975) 1253.
[2] A. Tauber, R.O. Savage, Jr., T. Collins, J. Mitchell, J.R. Shappiro and D.W. Eckatt, Proc. 23rd Ann. Conf. on Magnetism and Magnetic Materials (Minneapolis), Nov. 8–11, 1977, to be published.
[3] P.D. Baba, G.M. Argentina, W.E. Courtney, G.F. Dionne and D.H. Temme, IEEE Trans. Magn. Mag. 8 (1972) 83.
[4] G.M. Argentina and P.D. Baba, IEEE Trans. Microwave Theory Tech. 22 (1974) 654.
[5] J.J. Green and H.J. van Hook, IEEE Trans. Microwave Theory Tech. 25 (1977) 155.
[6] K.I. Arai and N. Tsuya, J. Phys. Soc. Japan 33 (1962) 1581.
[7] V.J. Folen, J. Appl. Phys. 31S (1960) 1665.
[8] G.A. Petrakovskii and L.M. Smokotin, Sov. Phys.-JETP 26 (1968) 718.
[9] R.G. West and A.C. Blankenship, J. Am. Ceram. Soc. 50 (1967) 343.
[10] D.H. Ridgley, H. Lessoff and J.D. Childress, J. Am. Ceram. Soc. 53 (1970) 304.
[11] Y.M. Yakovlev, M.A. Vinnik, E.V. Rubalskaya and B.L. Lapovok, Sov. Phys.-Solid State 12 (1970) 669.
[12] G.F. Dionne, J. Appl. Phys. 45 (1974) 3621.
[13] E.W. Gorter, Philips Res. Repts. 9 (1954) 295.
[14] G. Blasse, Philips Res. Repts. Suppl. No. 3 (1964) 90.
[15] Y. Yafet and C. Kittel, Phys. Rev. 87 (1952) 290.
[16] T.A. Kaplan, Phys. Rev. 119 (1960) 1460.
[17] S. Geller, J. Appl. Phys. 37 (1966) 1408.
[18] G.F. Dionne, J. Appl. Phys. 41 (1970) 4874.
[19] J.W. Young and J. Smit, J. Appl. Phys. 42 (1970) 2344.
[20] C.R. Abelido and R.B. Frankel, J. de Phys. 38 (1977) C1-135.
[21] N.S. Satya Murthy, M.G. Natera, S.I. Youssef and R.J. Begum, Phys. Rev. 181 (1969) 969.
[22] L.K. Leung, B.J. Evans and A.H. Morrish, Phys. Rev. B8 (1973) 29.
[23] G.A. Pettit and D.W. Forester, Phys. Rev. B4 (1971) 3912.
[24] G.T. Rado and V.J. Folen, J. Appl. Phys. 31 (1960) 62.
[25] E. Prince, J. de Phys. 25 (1964) 503.
[26] S. Chikazumi, Physics of Magnetism (Wiley, New York, 1966) Chaps. 7 and 8.
[27] K. Yosida and M. Tachiki, Prog. Theoret. Phys. (Kyoto) 17 (1957) 331.
[28] W.P. Wolf, Phys. Rev. 108 (1957) 1152.
[29] H. Callen and E. Callen, US Office of Naval Research, Tech. Rept. No. 25, August (1965).
[30] V.J. Folen and G.T. Rado, J. Appl. Phys. 29 (1958) 438.
[31] S. Geschwind, Phys. Rev. 121 (1961) 363.
[32] H.B. Callen and S. Shtrikman, Solid State Comm. 3 (1965) 5.
[33] G.F. Dionne, J. Appl. Phys. 40 (1969) 4486.
[34] A. Broese von Groenou, Philips Res. Repts. 21 (1966) 180.
[35] H.J. van Hook and G.F. Dionne, AIP Conf. Proc. No. 24 (1974) 487.

[36] M.A. Stel'mashenko, Sov. Phys.-Solid State 9 (1967) 1137.
[37] M. Tachiki, Progr. Theoret. Phys. (Kyoto) 23 (1960) 1055.
[38] E. Callen and H.B. Callen, Phys. Rev. 139 (1965) A455.
[39] R.R. Birss and E.D. Isaac, in: Magnetic Oxides, vol. 1, ed. D.J. Craik (Wiley, London, 1975) p. 289.
[40] A.P. Greifer, IEEE Trans. Magnetics 5 (1969) 744.
[41] J.B. Goodenough, Phys. Rev. 95 (1954) 917.
[42] A. Globus, "Magnetization Mechanisms and Specific Polycrystalline Properties in Soft Magnetic Materials", Spec. Rept. CNRS, Bellevue, France (1975).
[43] E.A. Schwabe and D.A. Campbell, J. Appl. Phys. 34 (1963) 1251.
[44] J.K. Galt, Bell System Tech. J. 33 (1954) 1023.
[45] J.F. Dillon and H.E. Earl, J. Appl. Phys. 30 (1959) 202.
[46] J.A. Baldwin, Jr., J. Appl. Phys. 38 (1967) 501.
[47] J.A. Baldwin, Jr., J. Appl. Phys. 39 (1968) 5982.
[48] L.J. Dijkstra and C. Wert, Phys. Rev. 79 (1950) 979.
[49] L. Néel, Cah. Phys. 25 (1944) 21.
[50] R.M. Bozorth, Ferromagnetism (Van Nostrand, New York, 1951) Chap. 13.
[51] H.J. Williams, R.C. Sherwood, M. Goertz and F.J. Schnettler, AIEE Trans. Communications and Electronics 72 (1952) 531.
[52] J.E. Knowles, Proc. Phys. Soc. (London) 75 (1970) 885.
[53] R. Gans, Ann. Phys. (Leipzig) 15 (1932) 28.
[54] G.F. Dionne, J. Appl. Phys. 40 (1969) 431.
[55] J.B. Goodenough, J. Appl. Phys. 36 (1965) 2432.
[56] J.D. Childress, J. Appl. Phys. 38 (1967) 1307.
[57] G.F. Dionne, IEEE Trans. Magnetics 7 (1971) 715.
[58] G.F. Dionne, IEEE Trans. Magnetics 10 (1974) 947.
[59] M. Sparks, Ferromagnetic Relaxation Theory (McGraw-Hill, New York, 1964).
[60] E.G. Spencer, D.A. Lepore and J.W. Nielsen, J. Appl. Phys. 39 (1968) 732.
[61] W.G. Nilsen, R.L. Comstock and J.P. Remeika, J. Appl. Phys. 37 (1966) 1224.
[62] R.L. White, Phys. Rev. Lett. 2 (1959) 465.
[63] I.K. Pukhov, G.A. Petrakovskii, U.N. Seleznev and A.D. Prokhorov, Bull. Acad. Sci. USSR 34 (1970) 832.
[64] G.A. Petrakovskii and V.N. Berzhanskii, Sov. Phys.-Solid State 13 (1971) 495.
[65] J.P. Sage, J. Phys. Chem. Solids 29 (1968) 2199.
[66] V.N. Berzhanskii and G.A. Petrakovskii, Bull. Acad. Sci. USSR 34 (1970) 889.
[67] E.G. Spencer and R.T. Denton, J. Appl. Phys. 35 (1964) 2633.
[68] D.A. Lepore, R.F. Belt and J.W. Nielsen, J. Appl. Phys. 38 (1967) 1421.
[69] R.E. Kaelberer, G.O. White and C.E. Patton, J. de Phys. 38 (1977) C1-255.
[70] E. Schlömann, AIEE Spec. Pub. T-91 (Proc. Conf. Magnetism and Magnetic Materials) (1956) 660.
[71] C.E. Patton, Phys. Rev. 179 (1969) 352.
[72] M. Konwicki and S. Makolagwa, J. de Phys. 38 (1977) C1-271.
[73] C.E. Patton, IEEE Trans. Magnetics 8 (1972) 433.
[74] Q.H.F. Vrehen, H.G. Beljers and J.G.M. Delau, IEEE Trans. Magn. Mag. 5 (1969) 617.
[75] R.E. Kaelberer and C.E. Patton, IEEE Trans. Magn. Mag. 13 (1977) 1230.
[76] E. Schlömann, J. de Phys. 32 (1971) C1-443.
[77] R.W. Babbitt and W. Wade, ECOM Final Report, Project C93-N0067-01-C9-CA, January (1976).
[78] L.A. Davydov, S.A. Poltnikov and M.F. Bryzhina, Sov. Phys.-Solid State 7 (1965) 596.
[79] D.S. McClure, J. Phys. Chem. Solids 3 (1957) 311.
[80] D.H. Rogers, R.W. Germann and R.J. Arnott, J. Appl. Phys. 36 (1965) 2338.
[81] G. Blasse, Philips Res. Repts. 20 (1965) 528.
[82] H.J. Van Hook and J.J. Green, Air Force Materials Laboratory, Air Force Systems Command, Tech. Rept. AFML-TR-74-146 (1974).
[83] F.K. Lotgering, J. Phys. Chem. Solids 25 (1964) 95.
[84] T. Collins and A.E. Brown, IEEE Trans. Magnetics 3 (1967) 513.
[85] E.V. Lebedeva, A.I. Pil'shchikov and E.K. Yur'eva, Sov. Phys.-Solid State 9 (1967) 237.
[86] L.M. Protopopova, G.A. Petrakovskii and E.V. Rubalskaya, Bull. Acad. Sci. USSR 36 (1972) 1110.
[87] S.K. Banerjee, P.D. Baba, B.J. Evans and S.S. Hafner, J. de Phys. 32 (1971) C1-145.
[88] M.P. Bunina, E.V. Lebedeva, A.I. Pil'shchikov and I.I. Silverstrovich, Sov. Phys.-Solid State 12 (1970) 341.
[89] K.D. Dugar-Zhabon, Porosh. Met. 11 (1971) 60.